Neuron
Article

Anatomical Coupling of Sensory and Motor Nerve Trajectory via Axon Tracking

Liang Wang,[1] Rüdiger Klein,[2] Binhai Zheng,[3] and Till Marquardt[1,*]
[1]Developmental Neurobiology Laboratory, European Neuroscience Institute (ENI-G), Grisebachstraße 5, 37077 Göttingen, Germany
[2]Department of Molecular Neurobiology, Max-Planck Institute of Neurobiology, Am Klopferspitz 18, 82152 München-Martinsried, Germany
[3]Department of Neurosciences, University of California San Diego, 9500 Gilman Drive, La Jolla, CA 92093-0691, USA
*Correspondence: t.marquardt@eni-g.de
DOI 10.1016/j.neuron.2011.06.021

SUMMARY

It is a long-standing question how developing motor and sensory neuron projections cooperatively form a common principal grid of peripheral nerve pathways relaying behavioral outputs and somatosensory inputs. Here, we explored this issue through targeted cell lineage and gene manipulation in mouse, combined with in vitro live axon imaging. In the absence of motor projections, dorsal (epaxial) and ventral (hypaxial) sensory projections form in a randomized manner, while removal of EphA3/4 receptor tyrosine kinases expressed by epaxial motor axons triggers selective failure to form epaxial sensory projections. EphA3/4 act non-cell-autonomously by inducing sensory axons to track along preformed epaxial motor projections. This involves cognate ephrin-A proteins on sensory axons but is independent from EphA3/4 signaling in motor axons proper. Assembly of peripheral nerve pathways thus involves motor axon subtype-specific signals that couple sensory projections to discrete motor pathways.

INTRODUCTION

Accurate behavioral outputs rely on spinal sensory-motor circuits that channel afferent feedback and efferent output pathways through a common principal grid of peripheral nerves. The anatomical basis of these circuits is established during embryonic and neonatal development when motor neurons and dorsal root ganglion (DRG) sensory neurons innervate discrete muscle and dermal targets, and become mono- or polysynaptically connected in the spinal cord via central afferent projections (Chen et al., 2003; Fitzgerald, 2005). While mechanisms governing central afferent connectivity have begun to emerge (Garcia-Campmany et al., 2010), insights into organizing principles underlying coordinate pathway and target selection during common deployment of motor and sensory axons—and functionally heterologous CNS projections in general—remain sparse.

Developing motor axons possess a high degree of autonomous targeting specificity, allowing them to actively seek and innervate discrete muscle targets from the outset (Landmesser, 2001). This involves transcriptional programs assigning motor neuron subtype identities that determine the responsiveness of motor axons toward instructive guidance cues on mesenchymal cells in their trajectory and target area (Bonanomi and Pfaff, 2010). Developing sensory axons, in contrast, appear to generally lack such rigid targeting specificities and may extend in a rather opportunistic manner along permissive tissue tracks (Frank and Westerfield, 1982; Honig et al., 1986; Scott, 1986). Moreover, several classical embryological manipulations that prevented motor, but not sensory, axon extension in frog and chick embryos were shown to trigger a failure of sensory muscle innervation (Hamburger, 1929; Honig et al., 1986; Landmesser and Honig, 1986; Scott, 1988; Swanson and Lewis, 1986; Taylor, 1944; Tosney and Hageman, 1989). In addition, transplantation experiments suggested that the ability of displaced sensory neurons to form segmentally appropriate projections depended on the presence of motor axons extending from relocated neural tube segments (Honig et al., 1986; Landmesser et al., 1983). These studies suggest that peripheral sensory projections are critically influenced by their interaction with preceding motor projections. However, the molecular mechanisms underlying these observations were unknown, while the actual relevance of the postulated axonal interactions remained controversial (Wang and Scott, 1999; Wenner and Frank, 1995).

Labeling experiments in chick showed that different types of developing peripheral projections segregate into discrete fascicles, suggesting an involvement of selective axon sorting mechanisms (Honig et al., 1998). We recently reported that establishment of peripheral nerve pathways in mouse involves heterotypic repulsive transaxonal interactions critical for assuring anatomical and functional segregation of motor and sensory nerve pathways (Gallarda et al., 2008). This involved redundant actions by the receptor tyrosine kinases EphA3 and EphA4 that repel motor growth cones from sensory axons expressing their cognate ephrin-A ligands. Eph family proteins generally act via engagement of membrane-linked ephrin proteins to elicit a range of cell contact-dependent bidirectional signaling events implicated in neural development, plasticity, and disease (Pasquale, 2008), including the development of motor projections in the hindlimb (Eberhart et al., 2002; Helmbacher et al., 2000; Kramer et al., 2006; Luria et al., 2008). However, whether motor axon-derived signals conversely influence sensory projections, and thereby determine the fundamental pattern of peripheral nerve pathways, remains to be addressed.

In the present study, we explored these issues through targeted cell lineage and gene manipulation in mouse, combined

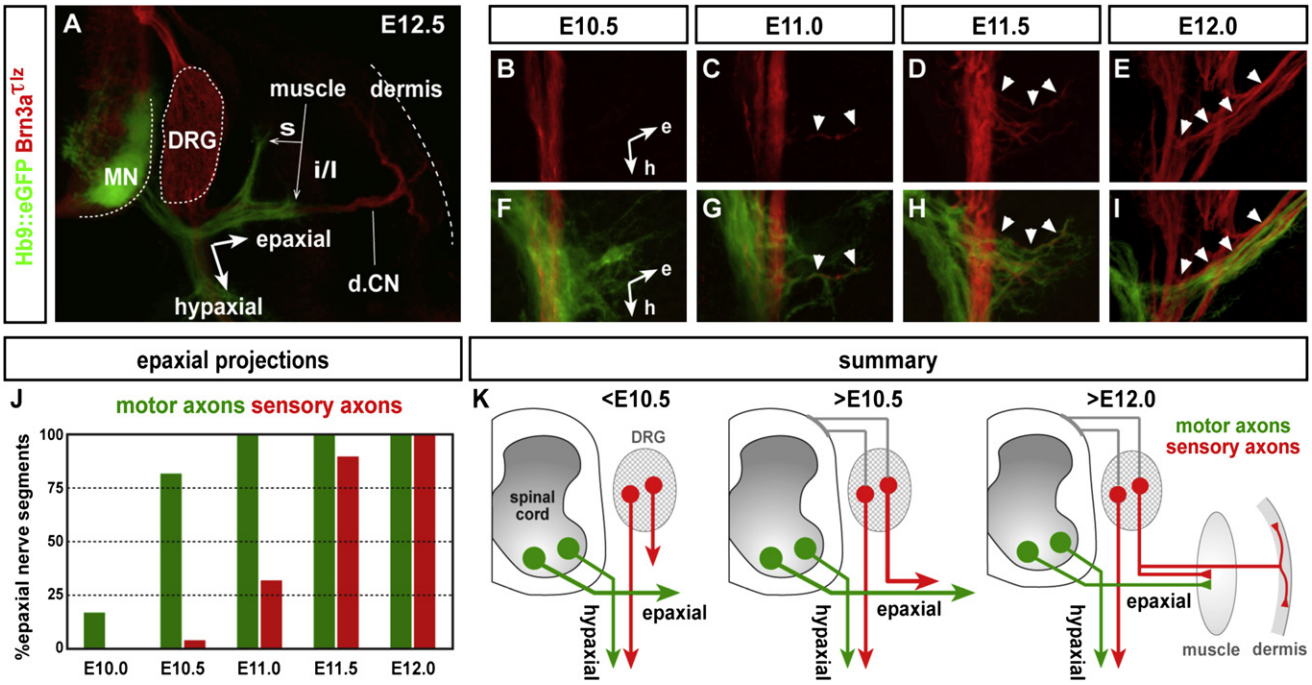

Figure 1. Epaxial sensory projections form along pre-extending motor axons

(A–I) Transversal sections (120 μm) at thoracic levels of mouse embryos. Developmental stages are indicated in embryonic days (E).

(A) Division of motor projections (green: Hb9::eGFP) and sensory projections (red: Brn3a$^{\tau lz}$) into epaxial and hypaxial trajectories (arrows) at E12.5. Abbreviations: DRG: dorsal root ganglion, MN: motor neurons, s: spinalis, i/l: iliocostalis/longissimus muscle nerves (thin arrows), dorsal cutaneous nerves (d.CN).

(B–I) Epaxial sensory projections (arrowheads) form after E10.5 in association with pre-extending motor axons. Arrows: division of epaxial (e) and hypaxial (h) trajectories.

(J) Quantitative summary: percentage of epaxial nerve segments with motor (green) and sensory projections (red) at indicated stages (E10.0: n = 13/3; E10.5: n = 19/3; E11.0: n = 19/2; E11.5: n = 23/2; E12.0: n = 45/2; number of sections/number of embryos).

(K) Schematic: epaxial sensory projections form along pre-extending motor axons. Note: both muscle and dermis-innervating sensory axons form in this manner.

with comprehensive tracing of genetically identified motor and sensory axons, as well as in vitro live axon imaging. We find that the establishment of normally patterned dorsal (epaxial) and ventral (hypaxial) sensory nerves relies on pre-extending motor projections. The formation of epaxial sensory projections specifically relies on non-cell-autonomous actions by EphA3 and EphA4 proteins on epaxial motor axons. EphA3/4 act by critically influencing sensory growth cone behaviors relative to preformed epaxial motor projections. This involves cognate ephrin-A proteins expressed by sensory axons but does not require EphA3/4 signaling in motor axons proper. These data provide conclusive evidence that assembly of peripheral nerve pathways involves motor axon subtype-specific signals that determine sensory axon trajectory relative to preformed motor projections.

RESULTS

Epaxial Sensory Projections Are Initiated along Preformed Motor Projections

To investigate whether interactions between coextending sensory and motor projections are involved in determining peripheral sensory trajectories, we first traced the normal development of both axon types in *Brn3a$^{tau:lacZ}$;Hb9::eGFP* double transgenic mice (Gallarda et al., 2008). Peripheral axons mainly extend along two principal avenues: the dorsal (epaxial) and ventral (hypaxial) rami, which at thoracic levels respectively innervate back and ventral trunk (Figure 1A). The first wave of axons exclusively extend hypaxially, but axons extending after embryonic day (E) 10.0 also project epaxially (Figures S1A and S1B, available online) (Shirasaki et al., 2006). We found that during both hypaxial and epaxial extension the first *Hb9::eGFP*-labeled (eGFP$^+$) motor axons invariably extended in advance of *Brn3a$^{tau:lacZ}$*-labeled (Tau:βGal$^+$) sensory axons (Figures S1A–S1E). Herein, motor axons first started to project epaxially after E10.0 (Figure 1B and Figures S1A–S1C), which was followed with a ~10 hr delay by the first epaxial sensory axons (Figures 1C). These sensory axons were always tightly associated with pre-extending motor axons (Figures 1C–1E). Codetection with the general axon marker βIII-tubulin confirmed that eGFP and Tau:βGal labeled the entire length of all initially extending motor and sensory projections, excluding the possibility that these observations reflected disparate axon labeling efficacies (Figures S1F–S1I). Do epaxial sensory projections form as collaterals from earlier hypaxial projections, or do they originate from a separate set of sensory neurons? Injection of retrograde axon tracers into hypaxial nerves consistently labeled hypaxial, but not epaxial,

projections (Figures S1P–S1U). This indicates that epaxial projections are formed de novo by a discrete set of later-extending axons, rather than trough interstitial branching from the same set of early-extending (hypaxial) axons. Taken together, the initial formation of peripheral projections proceeds according to the following pattern. First, axons begin extending from the hypaxial motor column along a hypaxial trajectory. Second, the first peripheral sensory axons extending from DRGs follow the pre-extending hypaxial motor axons. Third, with a delay, motor axons begin extending from the epaxial motor column to establish epaxial projections. Fourth, sensory axons continue extending from DRGs and now begin projecting epaxially in association with pre-extending epaxial motor axons (Figure 1K).

Division of Sensory Projections into Epaxial and Hypaxial Trajectories Depends on Preformed Motor Projections

We next asked whether preformed motor projections contribute to the establishment of peripheral sensory trajectories, by testing how sensory projections would develop in the absence of motor axons. To achieve this, we performed genetic ablation of motor neuron progenitors (pMNs) by generating $R26^{lox\text{-}DTA}$;$Olig2^{Cre}$ (*ΔpMN*) mouse embryos (Dessaud et al., 2010; Ivanova et al., 2005). In *ΔpMN* embryos, generation of spinal motor neurons and extension of motor axons was effectively prevented by *Cre/loxP* recombinase-mediated activation of cell-autonomously acting diphteria toxin in pMNs (compare Figures S2A–S2B and S2E–S2F). We did not detect any significant alteration in neuron numbers in the DRGs of *ΔpMN* embryos (Figure S2O, see also Figures S2B–S2D and S2F–S2H), while at all spinal segments DRG sensory axons extended peripherally in these embryos (compare Figures S2I and S2L). Thus, neither the principal generation of sensory neurons nor the initiation of peripheral sensory axon extension requires the presence of preformed motor neurons and motor axon projections. At the same time, however, the absence of motor projections in *ΔpMN* embryos resulted in a dramatically altered pattern of peripheral sensory axon projections that was particularly pronounced at thoracic levels (compare Figures 2A–2B and 2D–2E, see also Figures S2I to S2N). Instead of the normal bifurcation into epaxial and hypaxial trajectories, most thoracic nerve segments collapsed into a single epaxial or hypaxial sensory nerve in *ΔpMN* embryos (compare Figures 2C and 2F). This loss of either the hypaxial or epaxial trajectory was invariably accompanied by consistent increases in diameter of the nerve pathways remaining at affected segments (Figures 2G–2H and Figures S2P–S2Q). Without preformed motor pathways, the organization of peripheral sensory projections thus appears to desintegrate into the randomized "all-or-nothing" formation of either epaxial or hypaxial sensory pathways at the expense of the other (Figures 2J–2K). These data therefore reveal an absolute requirement of preformed motor projections for establishing the overall division of sensory projections into epaxial and hypaxial nerve trajectories.

Formation of Epaxial Sensory Projections Requires Motor Axonal EphA3/4

These observations suggested that the determination of peripheral sensory trajectories involves signals provided by epaxial and/or hypaxial motor axons, which prompted us to address the identity or identities of the putative signals. We have previously shown that epaxial motor axons display markedly higher levels of the receptor tyrosine kinases EphA3 and EphA4 compared to hypaxial motor axons (Gallarda et al., 2008). Moreover, contact-dependent activation of EphA3/4 on motor growth cones by their cognate ephrin-A proteins on sensory axons effectively repels developing epaxial motor axons from sensory pathways and DRGs (Gallarda et al., 2008). Since EphAs can also elicit "reverse" signaling by activating ephrin-As, we asked whether EphA3/4 could play additional roles in determining sensory projections (Egea and Klein, 2007; Pasquale, 2008). We therefore traced sensory projections in mouse embryos lacking both EphA3 and EphA4 (*Epha3/4*^{null}). *Epha3/4*^{null} embryos displayed severely defective formation of epaxial sensory pathways, while hypaxial projections formed normally (Figures S3E and data not shown).

We next asked whether the selective failure to form epaxial sensory projection in *Epha3/4*^{null} embryos involves EphA3/4 in motor neurons or in other cell types. To test this, we generated embryos in which the *Epha4* gene was selectively inactivated via *Cre/loxP*-mediated recombination in the motor neuron lineage of EphA3-deficient ($Epha3^{-/-}$) embryos (Figure S3A–S3D) (Herrmann et al., 2010). This strategy took advantage of the observation that any contribution of EphA3 to peripheral axon trajectories appears to be compensated as long as the functionally redundant EphA4 remains expressed (Figure S3F) (Gallarda et al., 2008; Vaidya et al., 2003). We further ruled out that the "floxed" *Epha4* allele (*Epha4*^{flox}) affected EphA4 function in the absence of Cre expression, by confirming that $Epha3^{-/-}$;$Epha4^{flox/flox}$ compound embryos did not show detectable peripheral projection defects (Figure S3F). We therefore concluded that the generation of $Epha3^{-/-}$;$Epha4^{flox/flox}$;$Olig2^{Cre}$ (*Epha3/4*$^{pMN\Delta flox}$) mice would allow us to selectively address the redundant activities of EphA3/4 in motor neurons/axons. *Epha3/4*$^{pMN\Delta flox}$ embryos displayed severely defective formation of epaxial sensory pathways (compare Figures 3A–3C and 3D–3F, see also Figures S3G and S3J). At the same time, hypaxial sensory pathways remained unaffected in these mutants (Figures S3I and 3L). Both the frequency and pattern of these epaxial sensory projection defects were virtually indistinguishable from those observed in *Epha3/4*^{null} embryos (Figure 3G). Because in *Epha3/4*^{null} embryos no alterations in DRG sensory neuron numbers were detected we could rule out that the selective epaxial projection defects in these mutants were caused by loss of a subset of sensory neurons (Figures S3N). Moreover, in both *Epha3/4*$^{pMN\Delta flox}$ and *Epha3/4*^{null} embryos the absence of epaxial sensory projections was further accompanied by a consistent increase in diameter of the hypaxial nerves (Figure 3H and Figures 3I–3L). This suggested that sensory projections that failed to extend epaxially instead grew hypaxially in these mutants (Figures 3M–3N).

We next tested whether these sensory projection defects were accompanied by similar defects in epaxial motor projections. Neither *Epha3/4*$^{pMN\Delta flox}$ nor *Epha3/4*^{null} embryos showed absence of epaxial motor projections, thus ruling out that the failure to form epaxial sensory projections was due to the loss of epaxial motor projections (compare Figures 3J and 3L; see

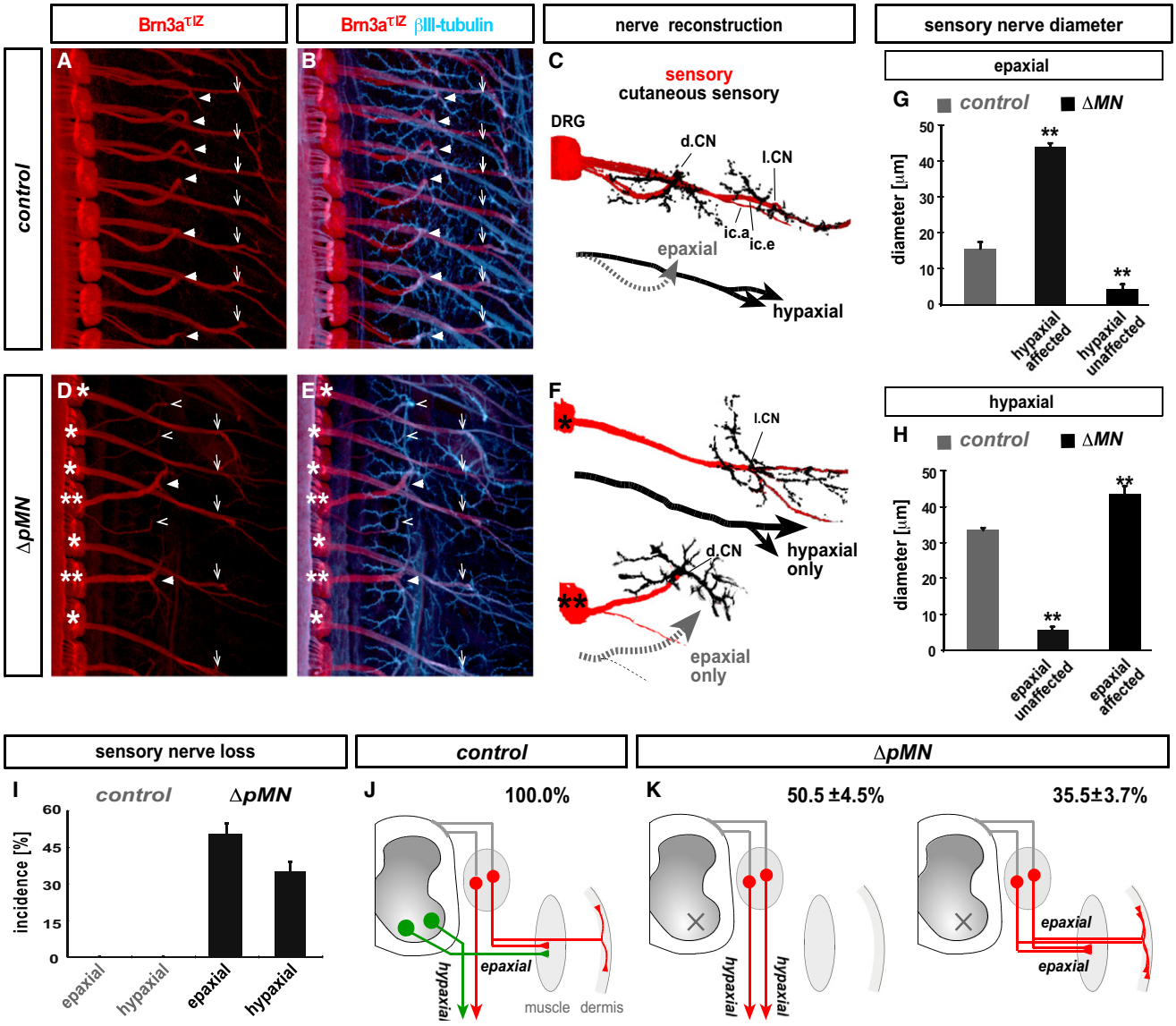

Figure 2. The Division of Sensory Projections into Epaxial and Hypaxial Pathways Requires Preformed Motor Projections

(A and B) Thoracic epaxial (arrowheads) and hypaxial sensory projections (vertical arrows) in whole-mounted E12.5 control embryo: visualized by Brn3a^{tlz} (red) and βIII-tubulin (blue).

(C) Graphical reconstruction of single nerve segment in control: overall division into epaxial (gray dotted arrow) and hypaxial sensory projections (black arrow). Cutaneous sensory arborizations are in black. Abbreviations: DRG: dorsal root ganglion, dorsal (d.CN), lateral cutaneous nerves (l.CN), anterior (ic.a), exterior intercostal ramus (ic.e).

(D and E) Absence of motor projections disrupts division of sensory projections into epaxial and hypaxial pathways (E12.5 whole-mounted *ΔpMN* embryo). Single asterisks: segments with absent/reduced epaxial, but expanded hypaxial projections. Double asterisk: segments with absent/reduced hypaxial, expanded epaxial projections. Open arrowheads: aberrant/reduced epaxial projections.

(F) Graphical reconstruction of two adjacent nerve segments in *ΔpMN* embryo reveals abnormal "all-or-nothing" formation of either hypaxial (top) or epaxial sensory projections (bottom).

(G and H) Quantification of epaxial (G) and hypaxial (H) nerve diameters. In *ΔpMN* embryos average nerve diameters were scored at segments classified as "affected" (reduced/absent) or "unaffected" (normal/expanded) (n = 120/5; n = 192/8; number of nerves/number of embryos, respectively). Data are presented as mean ± SEM. **p < 0.05 (Kruskal-Wallis test; see Supplemental Information).

(I) Quantification of overall epaxial and hypaxial nerve loss in control and *ΔpMN* embryos. Data are presented as mean ± SEM.

(J and K) Schematic summary: instead of the normal division into epaxial and hypaxial projections (J), absence of motor projections results in "all-or-nothing" formation of epaxial versus hypaxial sensory projections (K).

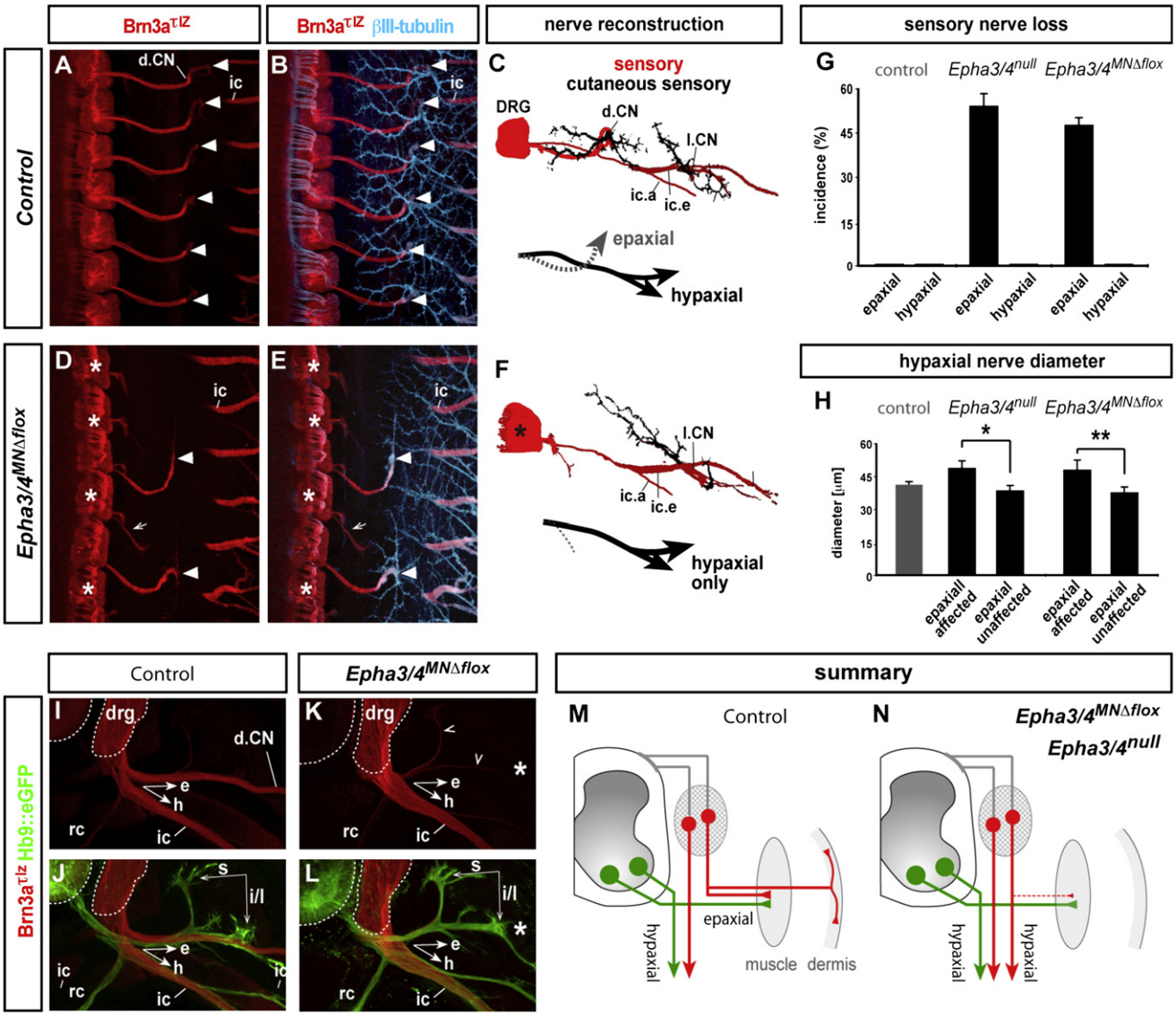

Figure 3. Formation of Epaxial Sensory Projections Depends on Motor Axonal EphA3/4 Proteins

(A and B) Thoracic epaxial sensory projections (arrowheads) in whole-mounted E12.5 control embryo.

(C) Graphical reconstruction of single nerve segment in control: overall division into epaxial (gray arrow) and hypaxial sensory trajectories (black arrow). Abbreviations as in Figure 2.

(D and E) Absence of EphA3/4 in motor neurons disrupts formation of epaxial sensory projections. Asterisks: segments with absent/reduced epaxial, but expanded hypaxial projections. Open arrows: aberrant/reduced epaxial projections.

(F) Graphical reconstruction of single nerve segment in *EphA3/4*$^{MN\Delta flox}$ embryo reveals selective loss of epaxial sensory projections.

(G) Quantification of overall epaxial or hypaxial nerve loss in control and *EphA3/4*$^{MN\Delta flox}$ embryos (n = 192/8; n = 120/5; n = 72/3; number of nerves/number of embryos, respectively). Data are presented as mean ± SEM.

(H) Hypaxial (intercostal) nerve diameter. Data are presented as mean ± SEM (*p = 0.034 < 0.05, **p = 0.041 < 0.05, student's t test; see Supplemental Information).

(I–L) Transversal thoracic sections (120 μm) at E12.5: epaxial (e) and hypaxial (h) sensory (red) and motor projections (green). Abbreviations as in Figures 1 and 2, apart from ic (intercostal nerve) and rc (ramus communicans).

(I and J) Normal bifurcation of epaxial and hypaxial sensory and motor projections.

(K and L) Severely reduced epaxial (asterisk, open arrowheads), but expanded hypaxial sensory projections. Epaxial motor projections are unaffected.

(M and N) Schematic summary: in the absence of motor axonal EphA3/4 sensory axons fail to project epaxially (N).

also Figures S3H and S3K). We next asked whether loss of epaxial sensory projections in these mutants could have been caused by hypaxial misrouting of epaxial motor axons. We tested this by retrogradely tracing of hypaxially projecting motor neurons by focal injection of fluorescent cholera toxin B (CtxB) into hypaxial intercostal nerves. In both control and *Epha3/4*^{null}

animals this effectively labeled hypaxial motor neurons residing within the lateral division of the medial motor column (MMCl) (Figures S3O–S3Q and S3R–S3T). At the same time, neither in control nor in *Epha3/4*^{null} embryos were epaxial motor neurons in the medial MMC (MMCm) labeled by hypaxial CtxB injection (Figures S3O–S3U). Thus, removal of motor axonal EphA3/4 selectively disrupts epaxial sensory projections, without resulting in the hypaxial misrouting of epaxial motor axons (Figures 3M–3N).

EphA3/4 Act Non-Cell-Autonomously to Determine Epaxial Sensory Projections

In addition to the sensory projection defects, both *Epha3/4*^{null} and *Epha3/4*$^{pMN\Delta flox}$ mutants display misrouting of epaxial motor axons into DRGs due to loss of repulsive EphA3/4 signaling in motor growth cones (data not shown) (Gallarda et al., 2008). We therefore asked whether the requirements of EphA3/4 for determining epaxial sensory projections could be uncoupled from their actions in repelling motor growth cones from DRGs. To address this, we tested how sensory projections would develop upon eliminating EphA3/4 repulsive intracellular signaling, while retaining the ability of motor axonal EphAs to engage their putative interaction partners on sensory axons. To achieve this, we generated embryos in which endogenous EphA4 is replaced by a signaling-deficient EphA4^{eGFP} chimeric protein in the absence of EphA3. In the corresponding *Epha3*$^{-/-}$;*Epha4*$^{eGFP/eGFP}$ (*Epha3/4*$^{\Delta kinase}$) mutants eGFP replaces the entire intracellular segment of EphA4 (Figure S4A), rendering the protein signaling deficient while preserving expression of its extracellular segment on epaxial motor axons (Figures S4B–S4J) (Grunwald et al., 2004). *Epha3/4*$^{\Delta kinase}$ embryos showed misrouting of motor projections into DRGs at a frequency similar to that observed in *Epha3/4*^{null} embryos (Figures S4K–S4N). In sharp contrast to *Epha3/4*^{null} animals, however, the vast majority of epaxial sensory projections formed normally in *Epha3/4*$^{\Delta kinase}$ embryos (Figures 4A–4G and Figure S4O–S4T). The EphA4 extracellular segment was therefore sufficient to allow formation of epaxial sensory projections in these embryos—despite the absence of EphA3/4 forward signaling and the associated misrouting of motor axons into DRGs (Figures 4H and 4I). EphA3/4 thus appear to act in a kinase-independent and non-cell-autonomous manner to determine epaxial sensory projections.

EphA3/4 Act through Cognate Ephrin-As to Determine Epaxial Sensory Projections

We next asked whether the determination of epaxial sensory projections by motor axonal EphA3/4 would involve their known interaction partners, the ephrins, on sensory axons. Affinity probe labeling experiments indicated that of the two classes of ephrins only the ephrin-As were present at substantial levels on DRG sensory neurons during the relevant development stages (Figures S5A–S5E). We therefore focused on the ephrin-As as possible sensory axonal binding partners for EphA3/4. Quantitative gene expression analysis showed that the mRNAs encoding several ephrin-As and EphAs were expressed in an overall complementary manner in sensory neurons and motor neurons, respectively (Figures S5F–S5G). In addition, the respective distribution of ephrin-A2 and EphA3/4 proteins on sensory and motor axons was consistent with facilitating interactions between ephrin-As on newly extending sensory axons, and EphA3/4 on pre-extending epaxial motor axons (Figures S5H–S5S). We therefore investigated the development of sensory projections in mice lacking the two major ephrin-As expressed in sensory neurons: ephrin-A2 and ephrin-A5 (Feldheim et al., 2000). In the *Efna2/5*^{null} mutants motor axons frequently misprojected into DRGs (Figures S5T and S5U). Loss of ephrin-A2/5 thus partially phenocopied the defective motor-sensory axon segregation observed in *Epha3/4*^{null} mutants (Figure S5V). Moreover, *Efna2/5*^{null} embryos displayed mild but persistent epaxial sensory projection defects (Figures S5W and S5X). In contrast to *Epha3/4*^{null} and *Epha3/4*$^{pMN\Delta flox}$ embryos, however, this was not accompanied by the loss of entire epaxial sensory nerve segments (data not shown). This suggested that additional ephrin-As or other potential EphA3/4-interaction partners compensated for the loss of ephrin-A2/5 on sensory axons.

We next reasoned that any impacts of lowering motor axonal EphA3/4 levels would likely be exacerbated by concomitantly reducing the availability of their putative interaction partners on sensory axons. We therefore monitored the development of sensory projections upon gradually lowering the levels of ephrin-A2/5 in mice with constant, but reduced EphA3/4 levels. Reduction of EphA3/4 levels in *Epha3*$^{+/-}$;*Epha4*$^{+/-}$ (*Epha3/4*^{het}) double heterozygous embryos was by itself not sufficient to trigger detectable alterations in sensory projections (Figures 5A–5B and Figure 5G). In contrast, the combined reduction of EphA3/4 and ephrin-A2/5 levels in *Epha3/4*^{het};*Efna2/5*^{het} compound embryos triggered consistent loss of epaxial sensory pathways (Figures 5C–5D and Figure 5G). Further reductions in ephrin-A2/5 levels in *Epha3/4*^{het} mice lead to increasingly pronounced loss of epaxial sensory projections (Figures 5E–5F and Figure 5G). These data therefore suggest that motor axonal EphA3/4 act at least in part through sensory neuron-expressed ephrin-As to determine epaxial sensory projections.

Sensory Axons Selectively Track along Epaxial Motor Projections

Our data so far indicate that the division of peripheral sensory projections into epaxial and hypaxial trajectories generally depends on preformed motor pathways, while determination of epaxial sensory projections specifically requires EphA3/4 on epaxial motor axons. We next asked how the motor axon-derived signals would act at the cellular level to determine sensory axon trajectories. To test this, we performed live monitoring of direct encounters between cultured sensory growth cones and pre-extending epaxial motor axons (Figure 6A). This was modeled on the encounter of late-extending sensory axons with pre-extending epaxial motor axons predicted to occur during development of epaxial sensory projections in vivo. As a control, we in parallel monitored sensory growth cones encountering pre-extending sensory axons (Figure 6B). In the control experiments, most sensory growth cones appeared to ignore the presence of other sensory axons, and freely crossed pre-extending sensory axon shafts (Figures 6C and 6E and Movie S1; see also Figure S6A). Upon encountering pre-extending motor axons, however, the sensory growth cones failed to cross

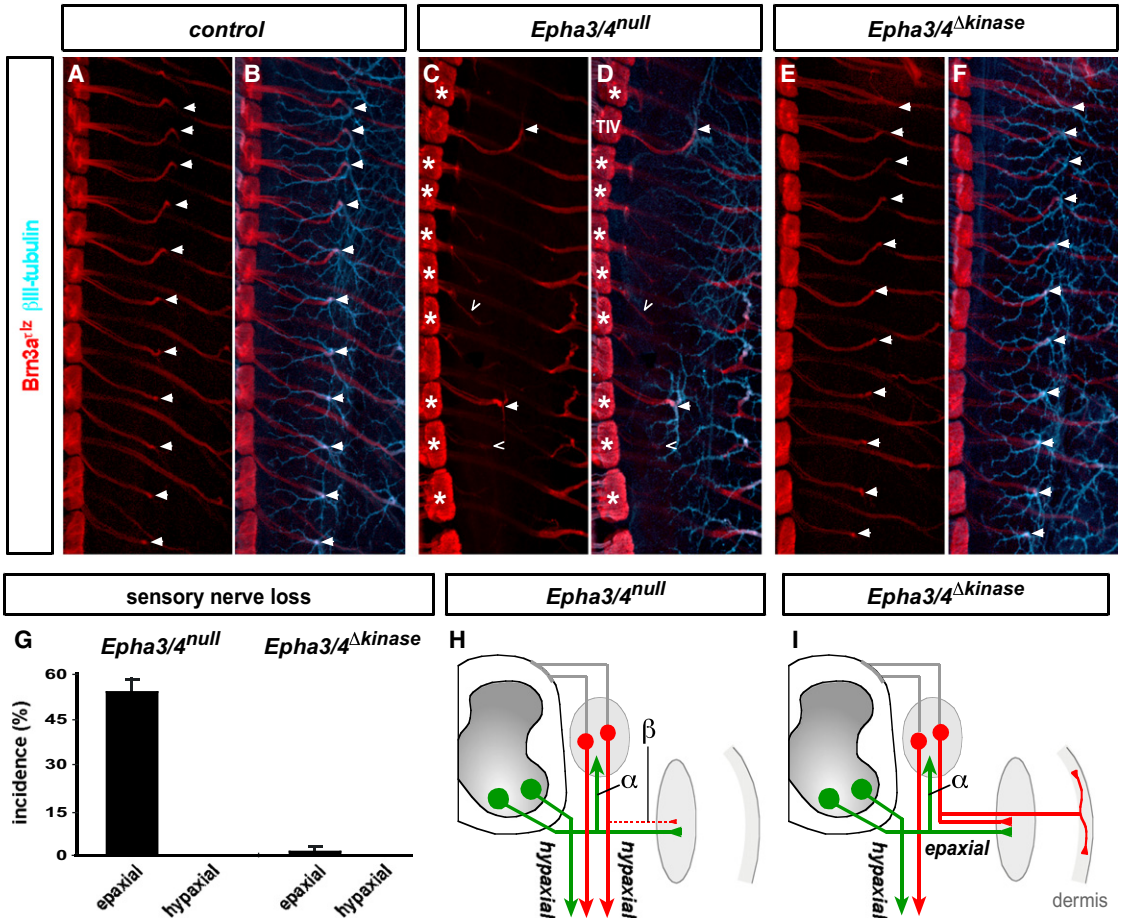

Figure 4. Reconstitution of EphA4 Ectodomain Expression Is Sufficient to Rescue Epaxial Sensory Projections in EphA3/4-Deficient Embryos

(A–F) Thoracic epaxial sensory projections (arrowheads) in whole-mounted E12.5 embryos.

(A and B) Normal pattern of epaxial sensory projections in control.

(C and D) Absence or severe reduction of several epaxial sensory projections in *EphA3/4*^{null} embryo (asterisks and open arrowheads).

(E and F) Most epaxial sensory projections form normally in *EphA3/4*$^{\Delta kinase}$ embryo.

(G) Quantification (percentage of nerve segments without epaxial/hypaxial sensory projections): near-normal formation of epaxial sensory projections in *EphA3/4*$^{\Delta kinase}$ embryos (n = 120/5; n = 144/6; number of nerves/number of embryos, respectively). Data are presented as mean ± SEM (Kruskal-Wallis test; see Supplemental Information).

(H and I) Summary: reconstitution of EphA4 ectodomain expression in *EphA3/4*$^{\Delta kinase}$ embryos rescued the loss of epaxial sensory projections (phenotype "β") observed in *EphA3/4*^{null} embryos. However, misprojections of epaxial motor axons into DRGs observed in *EphA3/4*^{null} embryos (phenotype "α": Gallarda et al., 2008) were not rescued in *EphA3/4*$^{\Delta kinase}$ embryos.

the interjecting axons and instead turned and began to track along the entire length of the motor projections (Figures 6D and 6F and Movie S2 and Movie S3). These behaviors were observed irrespective of the specific angle or velocity at which sensory axons encountered the motor axons (Figures S6E–S6G). Notably, sensory growth cones were observed to preferentially track toward the distal tip of the motor axon (Figure 6G). At the interface between sensory growth cone and motor axon, this was typically accompanied by the iterative cycling of transient sensory filopodia contact, retraction, and renewed extension events (Figure S6D and Movie S4). The tracking of sensory growth cones along motor axons therefore differed from the tight adhesive axon bundling typically associated with axon fasciculation. These data show that epaxial motor axons effectively induce sensory growth cones to follow pre-established motor projections in vitro, which suggested a cellular mechanism through which motor projections could determine peripheral sensory projections in vivo.

EphA3/4 Act through Cognate Ephrin-As to Induce Tracking of Sensory Projections along Epaxial Motor Projections

We next asked whether the epaxial sensory projection defects observed upon eliminating EphA3/4 could have resulted from altered behaviors of sensory axons toward epaxial motor axons. To test this, we monitored encounters of wild-type sensory growth cones with epaxial motor axons derived from control (*Epha3/4*^{het}) or *Epha3/4*^{null} embryos (Figure 7C). In contrast to

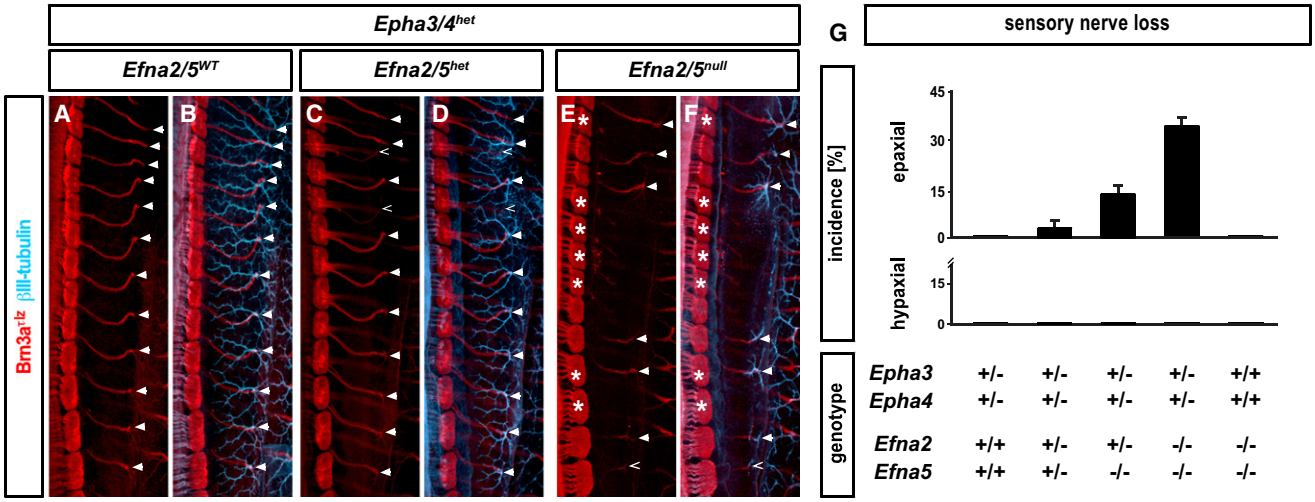

Figure 5. Genetic Evidence that EphA3/4 Act through Cognate Ephrin-As for Determining Epaxial Sensory Projections

(A–F) Thoracic epaxial sensory projections (arrowheads) in whole-mounted E12.5 embryos.

(A and B) Normal pattern of epaxial sensory projections in *Epha3/4*^{het} double heterozygous embryo.

(C and D) Sporadic epaxial sensory projection defects (open arrowheads) in *Epha3/4*^{het};*Efna2/5*^{het} quadruple heterozygous embryo.

(E and F) Frequent absence/severe reduction of epaxial sensory projections in *Epha3/4*^{het};*Efna2/5*^{null} compound mutant embryo (asterisks).

(G) Quantification: percentage of nerve segments without epaxial/hypaxial sensory projections in indicated genotypes. Frequency of epaxial sensory nerve loss increases with decreasing *Efna2/5* gene dosage (n = 96/4, n = 96/4; n = 120/5; n = 72/3; n = 96/4, respectively, number of nerves/number of embryos). Data are presented as mean ± SEM.

the control motor axons, most motor axons derived from *Epha3/4*^{null} embryos failed to induce tracking of wild-type sensory axons (compare Figures 7A–7B and Movie S5 and Movie S6). Instead, the encounter with EphA3/4-deficient motor axons frequently triggered collapse, retraction and eventual stalling of the sensory growth cones (Figures 7B and 7D–7E; see also Movie S6). Removal of EphA3/4 thus shifted the behavior of sensory growth cones toward epaxial motor axons from "tracking" to "avoidance," suggesting the presence of a motor axon-derived repulsive activity that is normally masked by EphA3/4. We next asked whether the altered sensory growth cone behavior toward EphA3/4-deficient motor axons was due to the loss of EphA3/4 ectodomains or was rather caused by adaptive changes in the motor axons due to loss of EphA3/4 intra-axonal signaling. We therefore tested whether EphA4 ectodomain expression in the absence of EphA3/4 signaling would be sufficient to restore the induction of sensory axon tracking. Consistent with the rescue of epaxial sensory projection defects in *Epha3/4*$^{\Delta kinase}$ embryos, *Epha3/4*$^{\Delta kinase}$ motor axons induced tracking of wild-type sensory growth cones comparable to control or wild-type motor axons (Figure 7F and data not shown). This suggested that sensory axon tracking depends on expression of EphA ectodomains on motor axons but does not require the activation of EphA3/4 signaling in motor axons proper. We next tested whether reduced ephrin-A expression on sensory axons would influence sensory growth cone behaviors toward wild-type motor axons. Sensory axons derived from *Efna2/5*^{null} embryos displayed diminished tracking and increased growth cone repulsion upon encounter with wild-type motor axons (Figures 7G and Figure S7E). Consistent with the comparatively mild sensory projection defects observed upon loss of ephrin-A2/5 in vivo, the shift in sensory axon behaviors was less pronounced in these experiments compared to those using *Epha3/4*^{null} motor axons (Figures 7E and 7G). We next asked whether concomitant reduction of motor axonal EphAs and sensory axonal ephrin-As would alter the behavior of sensory axons toward motor axons. Compared to control experiments, sensory axons derived from *Efna2/5*^{het} embryos displayed increased avoidance of motor axons derived from *Epha3/4*^{het} embryos (Figure S7D). Thus, motor axonal EphAs, and to a lesser extent sensory axonal ephrin-As, are critical for the ability of epaxial motor axons to recruit sensory axons along their pre-established trajectories.

EphA Ectodomains Promote Sensory Axon Extension in an Ephrin-A-Dependent Manner

Our data so far indicate that motor axonal EphA3/4 act in a non-cell-autonomous manner to determine sensory axon projections in vitro and in vivo. This prompted us to ask whether EphA proteins would directly influence sensory axon extension in a simplified in vitro environment. To test this, sensory axons were allowed to extend on control substrates or substrates containing recombinant EphA3 ectodomain (EphA3^{ECD}) or paralogous EphA7^{ECD} protein. Exposure to the EphA^{ECD}-containing substrates resulted in markedly enhanced sensory axon extension compared to the control substrates (Figures 8A and 8B). The activity of the EphA^{ECD} proteins on sensory axon extension was observed irrespective of whether nerve growth factor (NGF) or neurotrophin-3 (NT-3) was used as neurotrophic supplements (Figures 8A and 8B). This was consistent with the requirements of EphA3/4 observed by us in vivo, which comprised both NGF-dependent cutaneous and NT3-dependent muscle sensory projections. We next asked whether EphA^{ECD} would act through ephrin-As to promote sensory axon extension.

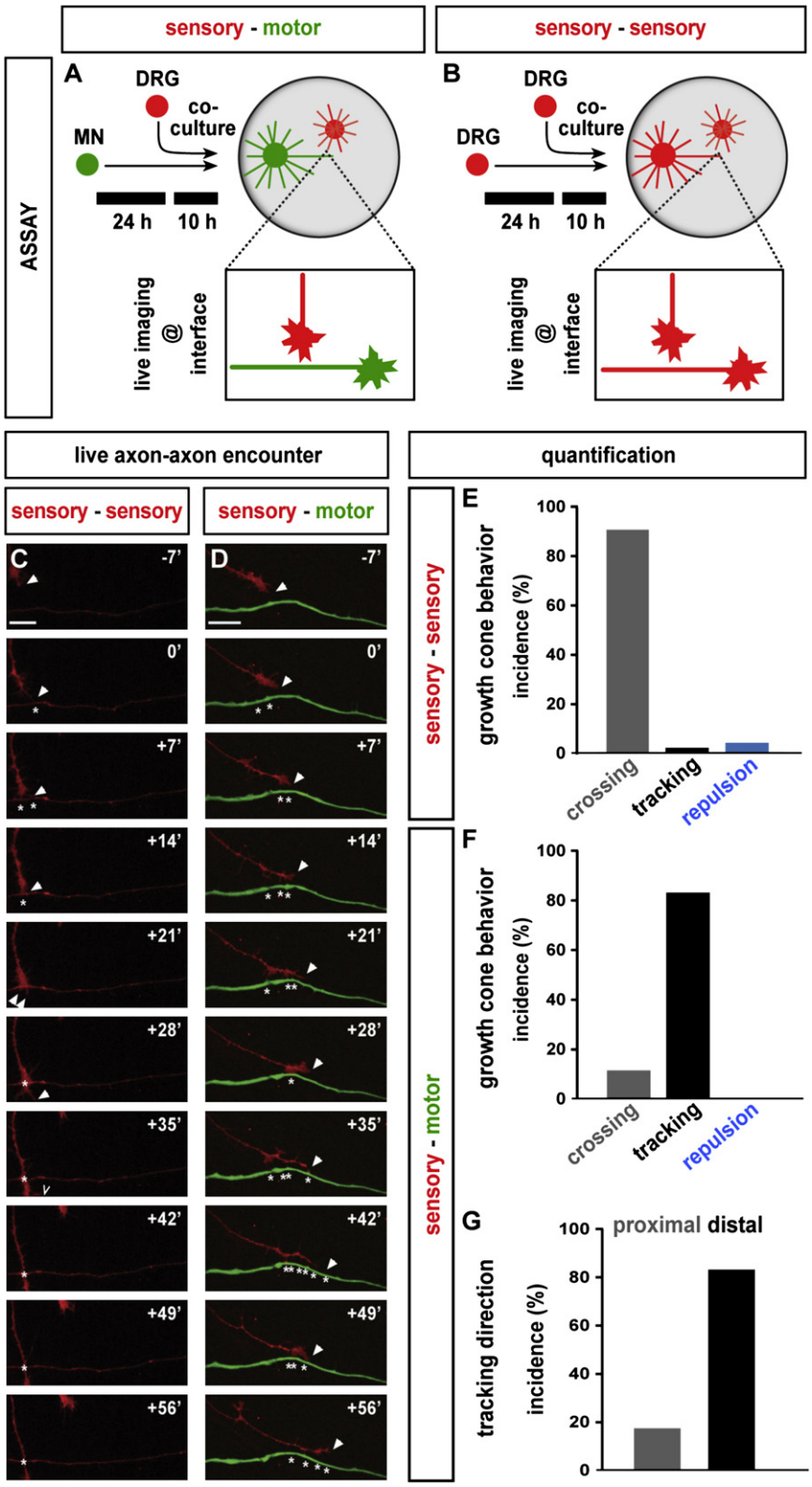

Figure 6. Sensory Axons Selectively Track along Preformed Motor Projections In Vitro

(A) Assay for monitoring interactions of sensory growth cones extending from cultured DRGs with motor axons pre-extending from cocultured motor neurons (MNs). See Supplemental Experimental Procedures.

(B) Assay for monitoring interactions of sensory growth cones with pre-extending sensory axons.

(C and D) Example time-lapse sequence of sensory growth cone/axon encounters. Indicated time: minutes prior (−) and after (+) initial contact (0) (Movie S2). Arrowheads indicate front of sensory growth cones.

(C) Sensory growth cone (red: DiI) crossing pre-extending sensory axon (asterisk) (see Movie S1).

(D) Sensory growth cone (red) encountering and tracking along pre-extending motor axon (green: Hb9::eGFP) (see Movie S2). Asterisks: sensory filopodial-motor axon contacts.

(E) Quantification of sensory growth cone-sensory axon interactions (n = 40/6 monitored encounters/number of experiments).

(F) Quantification of sensory growth cone-motor axon interactions (n = 43/12).

(G) Sensory growth cones preferentially track toward the distal motor axon tip (n = 38/6).

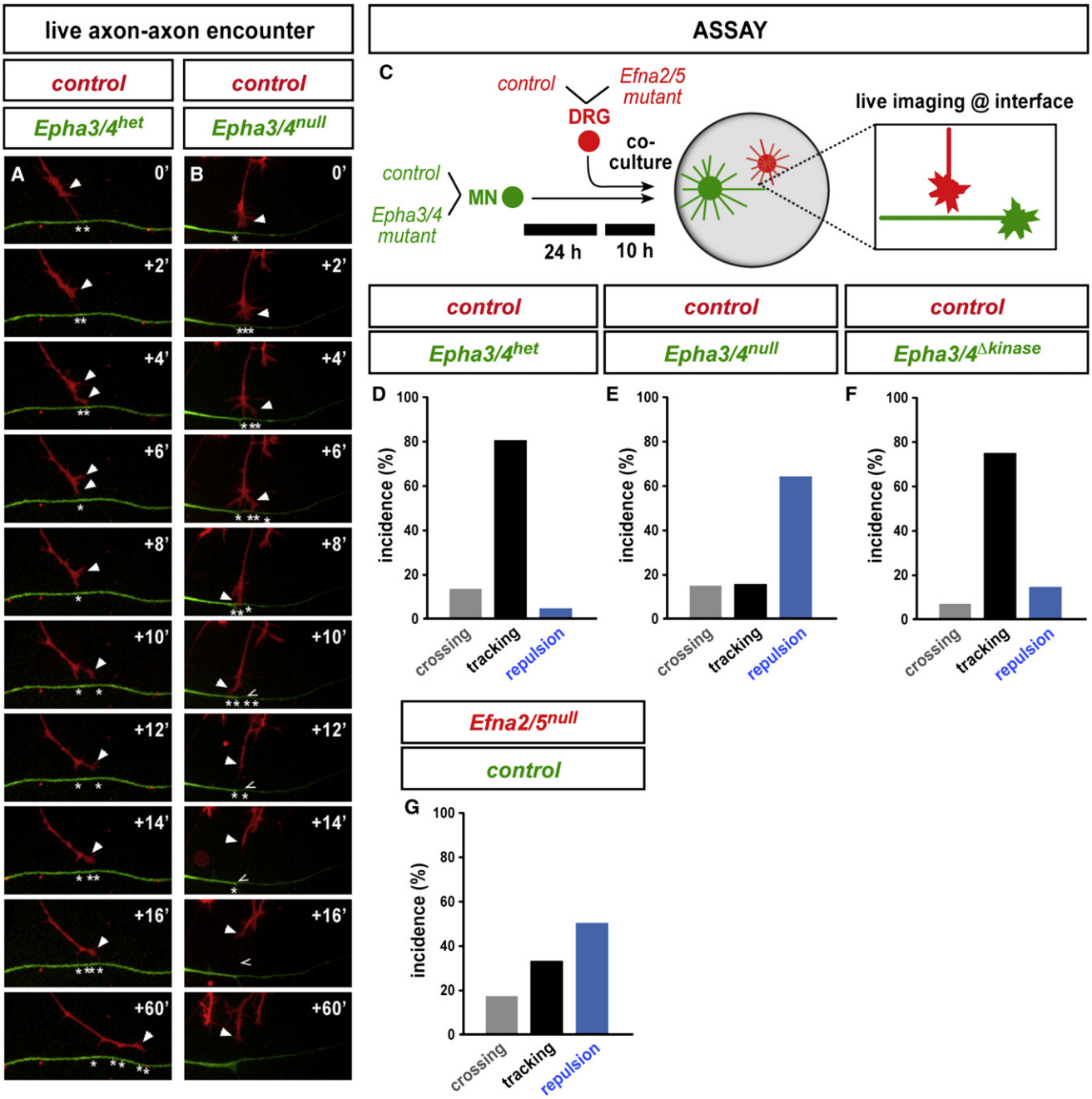

Figure 7. Tracking of Sensory Axons along Motor Axons Requires Motor Axonal EphAs and Sensory Axonal Ephrin-As

(A) Example time-lapse sequence of control (wild-type) sensory growth cones (red) tracking along *EphA3/4*^{het} motor axon (green) (Movie S5).

(B) Repulsion of wild-type sensory growth cone (red) from *EphA3/4*^{null} motor axon (green) (Movie S6). Asterisks: sensory filopodia-motor axon contacts. Closed arrowhead: front of sensory growth cone. Open arrowhead: delayed retraction of filopodial thread.

(C) Summary of assay for monitoring growth cone/axon interactions upon disrupting motor axonal EphA3/4 and/or sensory axonal ephrin-A2/5.

(D–G) Quantification of sensory growth cone/motor axon interactions. Genotypes of sensory axons and motor axons are indicated in red and green, respectively.

(D) Majority of control (wild-type) sensory growth cones track along *EphA3/4*^{het} motor axons (n = 18/10 monitored encounters/number of experiments).

(E) Most control sensory growth cone are repelled from *EphA3/4*^{null} motor axons (n = 42/8).

(F) Majority of control sensory growth cones track along *EphA3/4*$^{\Delta kinase}$ motor axons (n = 14/2).

(G) Many *Efna2/5*^{null} sensory growth cone are repelled from control (wild-type) motor axons (n = 8/4).

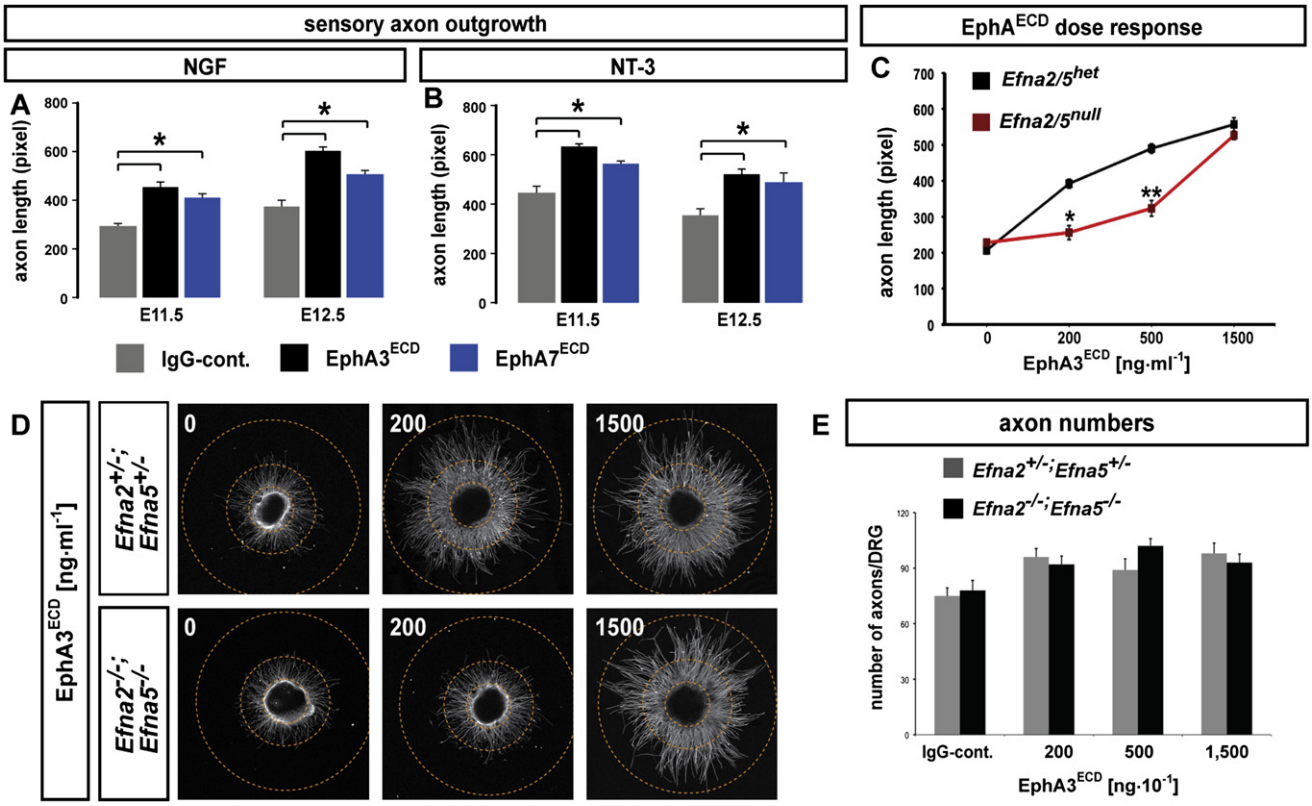

Figure 8. EphA Induce Sensory Axon Extension by Acting through Ephrin-As

(A and B) Recombinant EphA ectodomains (EphA^{ECDs}) promote sensory axon extension in vitro: axon length measured upon NGF (F), or NT-3 (G) selection in E11.5, E12.5 DRG sensory neurons cultured either on control protein (IgG) or EphA3^{ECD}, EphA7^{ECD}-containing substrates. Data are presented as mean ± SEM p* < 0.05 (Student's t test; see Supplemental Information).

(C) Lowered dose-response for EphA3^{ECD}-promoted axon outgrowth in *Efna2/5^{null}* sensory neurons. Data are presented as mean ± SEM. *p = 0.017 < 0.05, **p = 0.008 < 0.05 (Student's t test; see Supplemental Information).

(D) Examples of sensory axons extension from explanted DRGs: reduced of sensory axon-outgrowth responses toward EphA3^{ECD} in *Efna2/5^{null}*-derived sensory neurons.

(E) Quantitative summary of axon numbers in control (*Efna2$^{+/-}$;Efna5$^{+/-}$*) and *Efna2/5^{null}* (*Efna2$^{-/-}$;Efna5$^{-/-}$*) DRGs. Data are presented as mean ± SEM.

Sensory axons derived from *Efna2/5^{null}* embryos displayed significantly reduced extension in response to EphA3^{ECD} compared to control sensory axons (Figures 8C to 8E). Thus, EphA^{ECDs} are sufficient to promote sensory axon extension in vitro, at least in part by operating through sensory neuron-expressed ephrin-As.

DISCUSSION

The present study reveals an absolute requirement of motor axon-derived signals for establishing normally patterned peripheral sensory projections and provides mechanistic insights into the axonal interactions that couple peripheral sensory and motor pathways. Below, we discuss these findings in light of previous data by us and others.

Bidirectional Actions of Motor Axonal EphA3/4 in Peripheral Nerve Assembly

In a previous study we have shown that EphA3/4 contribute to the anatomical and functional segregation of epaxial motor projections from sensory pathways and DRGs (Gallarda et al., 2008). In *EphA3/4* null mutant embryos, epaxial motor axons misproject into proximal sensory pathways and DRGs, while electrophysiological recordings revealed that this results in the aberrant incorporation of motor input into sensory afferents. Sensory and/or motor neuron culture assays further showed that these phenotypes reflect a requirement for EphA3/4 repulsive signaling in motor growth cones, likely activated by their cognate ephrin-As on sensory axons (see Figures 9A–9A″). Herein, loss of EphA3/4 abolished motor growth cone repulsion induced by recombinant ephrin-A proteins or wild-type sensory axons in vitro (Gallarda et al., 2008). While these data established the central importance of heterotypic axon-axon interactions for the development of functionally segregated afferent and efferent pathways, the long-standing question of how sensory projections become aligned to preformed motor pathways remained unaddressed.

In the present study, we have tackled this issue by the extensive use of targeted cell lineage and conditional gene manipulation in mouse, combined with in vitro live axon imaging. First,

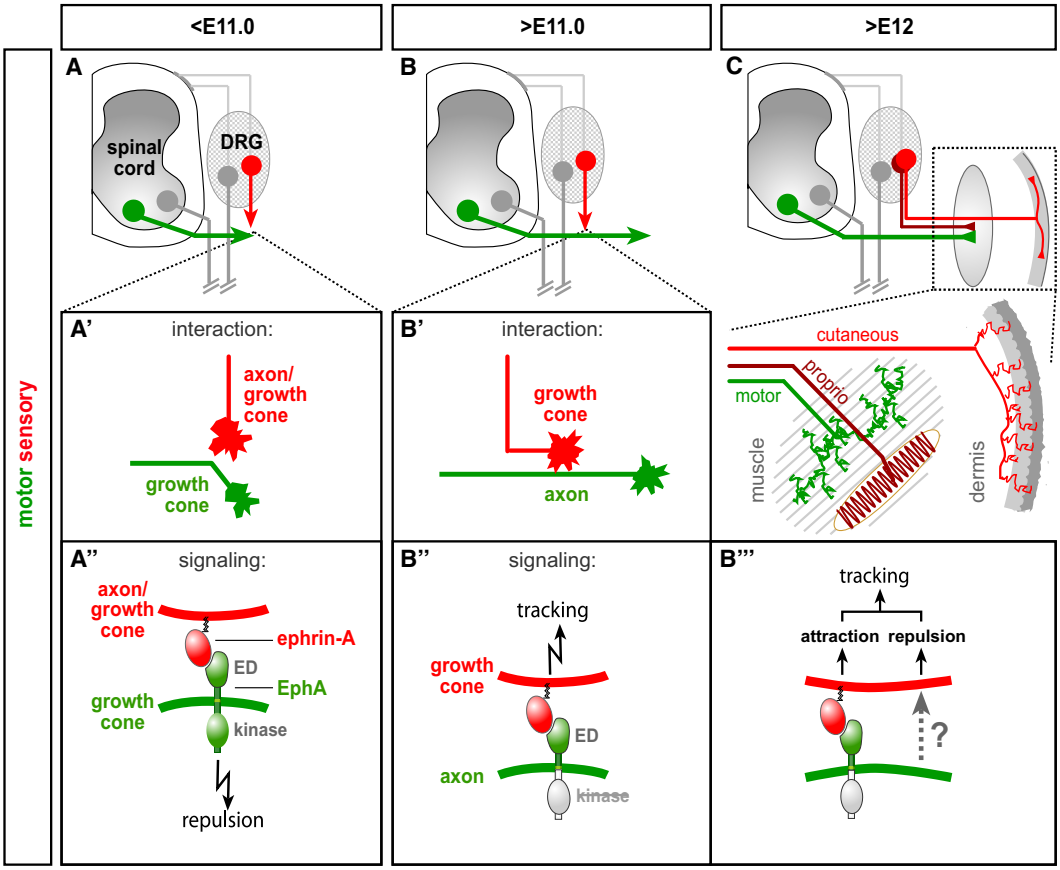

Figure 9. Model: Bidirectional Action of EphA3/4 during Epaxial Sensory-Motor Nerve Assembly

(A) Schematic: initial extension of epaxial motor axons (green) relative to sensory axons (red) in vivo. Earlier hypaxial projections are depicted in gray.

(A′) This stage facilitates interactions of epaxial motor growth cones with sensory axons, or sensory growth cones (see Figure S8A). Modeling of these interactions in vitro almost invariably triggers repulsion of the motor axon (see Figures S8C–S8D) (Gallarda et al., 2008).

(A″) Engagement of EphA3/4 by sensory axonal ephrin-As elicits repulsive *forward* signaling in motor growth cones requiring EphA3/4 kinase activity.

(B) Advanced extension of epaxial motor axons in vivo.

(B′) This stage favors interaction of late-extending sensory growth cones with motor axons. Modeling of these interactions in vitro results in tracking of sensory axon along pre-extending motor axon (see Figures S8E–S8F).

(B″) Model: engagement of ephrin-As (and possibly other molecules) on sensory growth cones by EphA3/4 on epaxial motor axons promotes tracking of sensory axons along pre-extending motor axons. This involves EphA3/4 kinase-independent *reverse* signaling.

(B‴) Detailed model: "attractive" reverse signaling activated by EphA3/4 on sensory growth cones is paralleled by an unknown motor axon-derived repulsive activity. Upon loss of EphA3/4 (or sensory axonal ephrin-As), this repulsive action shifts balance toward sensory growth cone repulsion.

(C) Advanced extension of epaxial sensory projections leads to innervation of muscle and dermis. Inset: cutaneous sensory axons eventually project beyond the proximal pathway shared with motor axons and proprioceptive sensory axons.

genetic manipulations that completely blocked motor projections triggered randomized formation of either epaxial or hypaxial sensory nerves. Second, conditional or systemic removal of motor axonal EphA3/4 triggered selective loss of epaxial sensory projections, while preserving epaxial motor projections. Third, subsequent gene replacement experiments in mice revealed that, intriguingly, the requirement of EphA3/4 for determining epaxial sensory projections operates independently from the EphA3/4 repulsive forward signaling involved in sensory-motor axon segregation. Herein, reconstituting EphA4 extracellular domain expression on epaxial motor axons in EphA3/4-deficient mice effectively rescued epaxial sensory projections, but not the misrouting of motor axons into DRGs triggered by the loss of EphA3/4 repulsive forward signaling. Fourth, in vivo genetic interaction data and in vitro experiments indicated that motor axonal EphAs act by reverse signaling through cognate ephrin-A binding partners on sensory growth cones. Fifth, live axon imaging revealed that motor axons pre-extending in vitro induced sensory growth cones to track along their trajectories. Sixth, these sensory growth cone tracking behaviors required EphA3/4 ectodomain expression on motor axons or ephrin-A2/5 expression on sensory axons, but did not require EphA3/4 signaling in motor axons proper. Seventh, recombinant EphA ectodomains were sufficient to induce sensory axon extension in vitro, which involved ephrin-A2/5 expressed by sensory axons.

EphA3/4 therefore fulfills two diametrically opposed functions during peripheral nerve assembly. Initially, EphA3/4 repulsive forward signaling assures the segregation of epaxial motor axons from proximal sensory pathways (Figures 9A–9A″) (Gallarda et al., 2008). Subsequently, EphA3/4 operate through the reverse activation of ephrin-As on sensory growth cones to couple sensory projections to epaxial motor pathways (Figures 9B–9B″) (this study). What determines whether kinase-dependent EphA3/4 forward signaling or kinase-independent EphA3/4 reverse signaling are elicited between epaxial motor and sensory axons? A key factor is likely the developmental status of epaxial motor axon extension relative to sensory projections, because it dictates the specific growth cone-axon encounters possible between epaxial motor and sensory axons (Figures S8A and S8B). Herein, the initial extension of epaxial motor axons is predicted to favor interactions of epaxial motor growth cones with sensory growth cones and axons extending from DRGs within the same spinal segment (Figure S8A). Careful modeling of these interactions in vitro showed that they almost invariably lead to collapse and retraction of the motor growth cones (Figures S8C–S8D and Movie S7; see also: Gallarda et al., 2008). Loss of EphA3/4 or EphA3/4 forward signaling renders epaxial motor growth cones insensitive to repulsion by sensory axonal ephrin-As and results in misprojection of epaxial motor axons into DRGs. The converse interaction of sensory growth cones with proximal segments of epaxial motor axons only becomes possible after the motor axons have projected further distally (Figure S8B). In vitro, these interactions prompt sensory growth cones to track along the pre-extending epaxial motor axons, without affecting the trajectory of the latter (Figures S8E and S8F). Coupling of sensory projections to epaxial motor axons in vitro and in vivo required EphA ectodomains on the motor axons, but were independent of repulsive EphA forward signaling.

In summary, we propose that the specific growth cone-axon shaft encounters possible for late-extending, but not early-extending, axons (and vice versa) determine whether EphA/ephrin signaling can be elicited in the forward or reverse direction (Figures 9A–9B). What underlies the different signaling outcomes in axon shafts versus growth cones? Guidance receptors commonly influence axon migratory direction by eliciting local changes in the growth cone, but rarely by primarily acting on the axon shaft (Dickson, 2002; McLaughlin and O'Leary, 2005). Herein, the asymmetric distribution of critical downstream effectors and cytoskeletal components seem to effectively confine the forward actions of more widely distributed receptors, such as ephrin-As or EphAs, to the growth cone. However, it also remains possible that the shift from forward repulsive to reverse permissive EphA/ephrin-A signaling involves modulatory components that differ between early- and late-extending axon populations. Context-dependent modulation of guidance receptors is frequently observed (Dickson, 2002; Egea and Klein, 2007), and minute alterations in the balance of intracellular messengers can convert growth cone repulsion to attraction (Nishiyama et al., 2003). Distinguishing between these possibilities will be facilitated by eventually defining the downstream and coreceptor components through which EphAs and ephrin-As signal in motor and sensory axons.

Motor Axon-Derived Signals Determine the Pattern of Sensory Projections

Several classical embryological studies suggested that normal formation of peripheral sensory projections requires the presence of pre-extending motor axons (Hamburger, 1929; Taylor, 1944; Honig et al., 1986; Landmesser and Honig, 1986; Swanson and Lewis, 1986; Scott, 1988; Tosney and Hageman, 1989). The molecular basis underlying these observations was unknown, however, while the relevance of the postulated axonal interactions remained controversial (Wang and Scott, 1999; Wenner and Frank, 1995). We propose that these contradictory findings were likely caused by a combination of technical limitations inherent to the surgical manipulations used by the previous studies, and the particular nature of the axonal interactions involved in peripheral nerve assembly. For instance, the patterns of sensory projections that we observe in our mouse models suggest that the interactions relevant for determining specific sensory axon trajectories are limited to a small set of pioneer axons. This is consistent with previous ultrastructural investigations suggesting that the first sensory axons extending peripherally in vivo preferentially associate with motor axons, or mesenchymal cells, while the growth cones of delayed-extending sensory axons preferentially associate with pre-extending sensory axons (Xue and Honig, 1999). Therefore, once a certain trajectory has been set by a small set of pioneer axons, the bulk of trailing sensory axons would project along these pioneer projections. The interaction with preformed motor projections may thus assure that the pioneer sensory axons are distributed along all peripheral nerve trajectories, instead of randomly entering only one possible trajectory. Without guidance by motor axons, the initial pattern of pioneer sensory projections that is followed by later-extending sensory axons would therefore result in the all-or-nothing formation of sensory nerves that we observe the absence of motor projections or motor axonal EphA3/4. These patterns encompassed the formation of sensory nerves with enlarged terminal arborizations adjacent to territories lacking segmental sensory innervation. The dermis in these embryos thus appeared continuously innervated by sensory axons, despite the lack of ~50% of nerve segments (see for instance Figure 2E). Due to limitations in previously available axon tracing methods the nerve patterns resulting from the absence of motor axons could thereby have been misinterpreted as normal formation of sensory projections. Moreover, the removal of most, but not all, motor projections in $Olig2^{Cre};Isl2^{flxDTA}$ mouse embryos resulted in largely normal sensory projections (L.W. and T.M., unpublished data). Thus, only a minor fraction of the normally developing motor projections appear to be sufficient to determine the overall pattern of sensory projections. Incomplete prevention of motor axon extension, combined with suboptimal axon tracing methods, could thereby have led previous investigators to underestimate the degree to which motor axon-derived signals shape peripheral sensory projections.

Determining Epaxial and Hypaxial Sensory Projections

Epaxial sensory projections constitute approximately one-third of the total sensory axons at a given thoracic nerve segment, prompting the question whether only a subset of sensory axons would be competent to project along $EphA3/4^{+}$ epaxial motor

axons. However, most available data so far suggest that developing sensory axons collectively lack the capacity to distinguish between different peripheral trajectories (Frank and Westerfield, 1982; Honig et al., 1986; Scott, 1986). Consistently, our data suggest that most sensory axons are equally competent to project along EphA3/4^{+} epaxial motor axons. How are the appropriate portions of epaxial and hypaxial sensory projections determined? A key factor for determining the numbers of sensory axons able to project epaxially is likely the delayed timing of epaxial motor axon extension. Since epaxial projections form only after a substantial portion of sensory axon have already extended hypaxially, the delayed timing of epaxial motor projections effectively restricts the numbers of sensory growth cones able to interact with pre-extending epaxial motor axons from the outset. The timing of epaxial motor axon extension may itself be determined by the specific kinetics of FGF receptor signaling (Shirasaki et al., 2006).

EphA-Dependent and -Independent Signaling in Peripheral Nerve Assembly

Removal of EphA3/4 from epaxial motor axons prompted sensory axons to exclusively project hypaxially at ~50% of the nerve segments. This suggests that EphA3/4 on epaxial motor axons is normally required to actively incite late-extending sensory axons away from their default hypaxial trajectory and further suggests the presence of additional EphA3/4-independent activities on motor axons. Whether these activities are specific to hypaxial motor axons or whether EphA3/4 is superimposed on activities common to all motor axons remains to be explored. Another factor contributing to the failure of epaxial sensory projections could be the observed switch to sensory growth cone repulsion triggered by EphA3/4-deficient epaxial motor axons in vitro (Figure 9B‴). Moreover, the actions of EphA3/4 are likely paralleled by mechanisms that regulate the overall degree of fasciculation between peripheral axons (Honig et al., 1998). The assembly of peripheral sensory-motor pathways thus may involve a fine balance of several attractive and repulsive signals. This in turn could be important for consolidating the anatomical coupling of sensory projections to discrete motor projections with the necessary functional segregation of afferent and efferent pathways. The developmental wiring of central nervous system (CNS) circuitries in general entails assembly of nerve pathways comprising vast arrays of functionally disparate axon projections. A similar balance of repulsive and attractive transaxonal mechanisms could therefore represent a more widely employed strategy during assembly of CNS nerve pathways and circuitries.

EXPERIMENTAL PROCEDURES

Mouse models

All mouse work conformed regulations by the UMG animal welfare committee and German animal welfare laws. Mouse lines and embryos carrying discrete or compound gene modifications were generated through interbreeding. See Supplemental Information for complete description of lines and genotyping primers.

Immunohistochemistry

Immunodetection on 30–120 μm frozen sections or explants was performed as described (Gallarda et al., 2008; Marquardt et al., 2005). For immunodetection on > 180 μm floating sections primary antibody incubation was in 1% BSA/PBS-T (0.5% Triton X-100) for ≥ 20 hr, secondary antibodies for ≥ 12 hr. For whole-mount immunodetection, E12.5 embryos were eviscerated in phosphate buffered saline (PBS, pH = 7.2), flat-mounted on 12-well plates (Nunc) on ice for ≥ 1 hr, and fixed at 4°C in 4% paraformaldehyde (PFA)/PBS and Dent's solution (Methanol:DMSO 4:1) for 12 hr and 6 hr, respectively, followed by ≥ 5 hr rehydration in PBS. Primary antibodies were incubated for 36–48 hr, secondary antibodies for 12–24 hr. Prior to microscopy, embryos were cleared in BABB. See Supplemental Information for a list of antibodies used.

Microscopy and Image Analysis

Images of fixed sections and whole embryos were collected using a Leica TCS/MP confocal/two-photon microscope or an Olympus Fluoview FV1000 laser scanning microscope (courtesy of Olympus-Deutschland GmbH).

Live Axon Imaging

Fluorescence-guided microdissection and culture of MMCm and DRG explants were carried out as described (Gallarda et al., 2008). Live axon imaging was initiated prior to first sensory growth cone-motor axon contact using an Olympus Cell^M Yokogawa DSU-based spinning disk system, plus mounted incubator chamber. Live sequences were documented by a Hamamatsu CCD camera and converted to time-lapse sequences using the Cell^M work station.

Sensory Neurite Outgrowth Assay

Neurite outgrowth assays on E11.5–12.5 mouse DRGs was essentially performed as described (Marquardt et al., 2005), adjusted to minimal neurotrophin requirements of DRG sensory neurons (0.1 ng × ml^{-1} NGF, 1.5 ng × ml^{-1} NT-3, R&D systems, Sigma). Anti-Fc (Jackson IR) preclustered IgG, EphA3^{ECD}, and EphA7^{ECD} (R&D) were conjugated with 5.0 μg × ml^{-1} laminin (Sigma) on PDL coverslips (BD Bioscience) at 4°C overnight.

SUPPLEMENTAL INFORMATION

Supplemental Information includes eight figures, one table, complete Experimental Procedures, and seven movies and can be found with this article online at doi:10.1016/j.neuron.2011.06.021.

ACKNOWLEDGMENTS

We thank A. Klusowski and E. Ling for technical assistance and D. Müller and A. Kania for comments on the manuscript. We are indebted to B. Novitch and T.M. Jessell for providing *Olig2^{Cre}* mice and to D. Feldheim for *Efna2/5^{null}* mice. We further thank G. Lemke and A. Brown for *Epha3^{null}* mice, E. Turner for *Brn3a$^{tau:lacZ}$* mice, L.F. Reichardt for anti-TrkC, and S.L. Pfaff for Isl1/2, Lhx3 antibodies, as well as S. Eimer and D.W. Richter for support obtaining the Cell^M system and Olympus-Germany for providing the DSU. This work was supported by the Emmy Noether Program of the Deutsche Forschungsgemeinschaft (DFG), as well as the DFG Research Center for Molecular Physiology of the brain (CMPB). B.Z. was funded by NIH/NINDS (R01NS054734) and a Roman Reed Fund. The ENI-G is a cooperation of the University of Göttingen Medical School (UMG) and the Max-Planck Gesellschaft.

Accepted: June 14, 2011
Published: July 27, 2011

REFERENCES

Bonanomi, D., and Pfaff, S.L. (2010). Motor axon pathfinding. Cold Spring Harb. Perspect. Biol. *2*, a001735.

Chen, H.H., Hippenmeyer, S., Arber, S., and Frank, E. (2003). Development of the monosynaptic stretch reflex circuit. Curr. Opin. Neurobiol. *13*, 96–102.

Dessaud, E., Ribes, V., Balaskas, N., Yang, L.L., Pierani, A., Kicheva, A., Novitch, B.G., Briscoe, J., and Sasai, N. (2010). Dynamic assignment and

maintenance of positional identity in the ventral neural tube by the morphogen sonic hedgehog. PLoS Biol. *8*, e1000382.

Dickson, B.J. (2002). Molecular mechanisms of axon guidance. Science *298*, 1959–1964.

Eberhart, J., Swartz, M.E., Koblar, S.A., Pasquale, E.B., and Krull, C.E. (2002). EphA4 constitutes a population-specific guidance cue for motor neurons. Dev. Biol. *247*, 89–101.

Egea, J., and Klein, R. (2007). Bidirectional Eph-ephrin signaling during axon guidance. Trends Cell Biol. *17*, 230–238.

Feldheim, D.A., Kim, Y.I., Bergemann, A.D., Frisén, J., Barbacid, M., and Flanagan, J.G. (2000). Genetic analysis of ephrin-A2 and ephrin-A5 shows their requirement in multiple aspects of retinocollicular mapping. Neuron *25*, 563–574.

Fitzgerald, M. (2005). The development of nociceptive circuits. Nat. Rev. Neurosci. *6*, 507–520.

Frank, E., and Westerfield, M. (1982). The formation of appropriate central and peripheral connexions by foreign sensory neurones of the bullfrog. J. Physiol. *324*, 495–505.

Gallarda, B.W., Bonanomi, D., Müller, D., Brown, A., Alaynick, W.A., Andrews, S.E., Lemke, G., Pfaff, S.L., and Marquardt, T. (2008). Segregation of axial motor and sensory pathways via heterotypic trans-axonal signaling. Science *320*, 233–236.

Garcia-Campmany, L., Stam, F.J., and Goulding, M. (2010). From circuits to behaviour: motor networks in vertebrates. Curr. Opin. Neurobiol. *20*, 116–125.

Grunwald, I.C., Korte, M., Adelmann, G., Plueck, A., Kullander, K., Adams, R.H., Frotscher, M., Bonhoeffer, T., and Klein, R. (2004). Hippocampal plasticity requires postsynaptic ephrinBs. Nat. Neurosci. *7*, 33–40.

Hamburger, V. (1929). Experimentelle Beiträge zur Entwicklungsphysiologie der Nervenbahnen in der Forschextremität. Rouxs Arch. Dev. Biol. *119*, 47–99.

Helmbacher, F., Schneider-Maunoury, S., Topilko, P., Tiret, L., and Charnay, P. (2000). Targeting of the EphA4 tyrosine kinase receptor affects dorsal/ventral pathfinding of limb motor axons. Development *127*, 3313–3324.

Herrmann, J.E., Pence, M.A., Shapera, E.A., Shah, R.R., Geoffroy, C.G., and Zheng, B. (2010). Generation of an EphA4 conditional allele in mice. Genesis *48*, 101–105.

Honig, M.G., Lance-Jones, C., and Landmesser, L. (1986). The development of sensory projection patterns in embryonic chick hindlimb under experimental conditions. Dev. Biol. *118*, 532–548.

Honig, M.G., Frase, P.A., and Camilli, S.J. (1998). The spatial relationships among cutaneous, muscle sensory and motoneuron axons during development of the chick hindlimb. Development *125*, 995–1004.

Ivanova, A., Signore, M., Caro, N., Greene, N.D., Copp, A.J., and Martinez-Barbera, J.P. (2005). In vivo genetic ablation by Cre-mediated expression of diphtheria toxin fragment A. Genesis *43*, 129–135.

Kramer, E.R., Knott, L., Su, F., Dessaud, E., Krull, C.E., Helmbacher, F., and Klein, R. (2006). Cooperation between GDNF/Ret and ephrinA/EphA4 signals for motor-axon pathway selection in the limb. Neuron *50*, 35–47.

Landmesser, L.T. (2001). The acquisition of motoneuron subtype identity and motor circuit formation. Int. J. Dev. Neurosci. *19*, 175–182.

Landmesser, L., and Honig, M.G. (1986). Altered sensory projections in the chick hind limb following the early removal of motoneurons. Dev. Biol. *118*, 511–531.

Landmesser, L.T., O'Donovan, M.J., and Honig, M. (1983). The response of avian hindlimb motor and sensory neurons to an altered periphery. Prog. Clin. Biol. Res. *110* (Pt A), 207–216.

Luria, V., Krawchuk, D., Jessell, T.M., Laufer, E., and Kania, A. (2008). Specification of motor axon trajectory by ephrin-B:EphB signaling: symmetrical control of axonal patterning in the developing limb. Neuron *60*, 1039–1053.

Marquardt, T., Shirasaki, R., Ghosh, S., Andrews, S.E., Carter, N., Hunter, T., and Pfaff, S.L. (2005). Coexpressed EphA receptors and ephrin-A ligands mediate opposing actions on growth cone navigation from distinct membrane domains. Cell *121*, 127–139.

McLaughlin, T., and O'Leary, D.D. (2005). Molecular gradients and development of retinotopic maps. Annu. Rev. Neurosci. *28*, 327–355.

Nishiyama, M., Hoshino, A., Tsai, L., Henley, J.R., Goshima, Y., Tessier-Lavigne, M., Poo, M.M., and Hong, K. (2003). Cyclic AMP/GMP-dependent modulation of Ca^{2+} channels sets the polarity of nerve growth-cone turning. Nature *423*, 990–995.

Pasquale, E.B. (2008). Eph-ephrin bidirectional signaling in physiology and disease. Cell *133*, 38–52.

Scott, S.A. (1986). Skin sensory innervation patterns in embryonic chick hindlimb following dorsal root ganglion reversals. J. Neurobiol. *17*, 649–668.

Scott, S.A. (1988). Skin sensory innervation patterns in embryonic chick hindlimbs deprived of motoneurons. Dev. Biol. *126*, 362–374.

Shirasaki, R., Lewcock, J.W., Lettieri, K., and Pfaff, S.L. (2006). FGF as a target-derived chemoattractant for developing motor axons genetically programmed by the LIM code. Neuron *50*, 841–853.

Swanson, G.J., and Lewis, J. (1986). Sensory nerve routes in chick wing buds deprived of motor innervation. J. Embryol. Exp. Morphol. *95*, 37–52.

Taylor, A. (1944). Selectivity of nerve fibers from the dorsal and ventral roots in the development of the frog limb. J. Exp. Zool. *96*, 159–185.

Tosney, K.W., and Hageman, M.S. (1989). Different subsets of axonal guidance cues are essential for sensory neurite outgrowth to cutaneous and muscle targets in the dorsal ramus of the embryonic chick. J. Exp. Zool. *251*, 232–244.

Vaidya, A., Pniak, A., Lemke, G., and Brown, A. (2003). EphA3 null mutants do not demonstrate motor axon guidance defects. Mol. Cell. Biol. *23*, 8092–8098.

Wang, G., and Scott, S.A. (1999). Independent development of sensory and motor innervation patterns in embryonic chick hindlimbs. Dev. Biol. *208*, 324–336.

Wenner, P., and Frank, E. (1995). Peripheral target specification of synaptic connectivity of muscle spindle sensory neurons with spinal motoneurons. J. Neurosci. *15*, 8191–8198.

Xue, Y., and Honig, M.G. (1999). Ultrastructural observations on the expression of axonin-1: implications for the fasciculation of sensory axons during axonal outgrowth into the chick hindlimb. J. Comp. Neurol. *408*, 299–317.